

論文 / 著書情報  
Article / Book Information

Title	Control of Radiation Direction in an Aperture Array Excited by a Waveguide 2-Plane Hybrid Coupler
Authors	Yuki SUNAGUCHI, Takashi TOMURA, Jiro HIROKAWA
Citation	IEICE TRANSACTIONS on Communications, vol. E105-B, no. 8, pp. 906-912
Pub. date	2022, 8
Copyright	Copyright(C)2022 IEICE

## PAPER

# Control of Radiation Direction in an Aperture Array Excited by a Waveguide 2-Plane Hybrid Coupler

Yuki SUNAGUCHI<sup>†a)</sup>, Takashi TOMURA<sup>†</sup>, Members, and Jiro HIROKAWA<sup>†</sup>, Fellow

**SUMMARY** This paper details the design of a plate that controls the beam direction in an aperture array excited by a waveguide 2-plane hybrid coupler. The beam direction can be controlled in the range of  $\pm 15$ – $32$  deg. in the quasi H-plane, and  $\pm 26$ – $54$  deg. in the quasi E-plane at the design frequency of 66.425 GHz. Inductive irises are introduced into tapered waveguides in the plate and the reflection is suppressed by narrow apertures. A plate that has a larger tilt angle in the quasi E-plane and another plate with conventional rectangular waveguide ports as a reference are fabricated and measured. The measured values agree well with the simulation results.  
**key words:** waveguide 2-plane coupler, hybrid junction, radiation direction, diffraction suppression, reflection suppression

## 1. Introduction

Spatial division multiple access (SDMA) [1] represented by massive MIMO (Multiple-Input and Multiple-Output) [2], [3] is an important methodology of multiplexing for enhancing the channel capacity. In order to implement an SDMA system, several types of beam scanning technologies can be used: phase scanning, frequency scanning, time delay scanning, and beam switching scanning.

The Butler matrix is one of the multibeam forming networks. Basically, a Butler matrix has  $2^n$  input ports and  $2^n$  output ports where  $n$  is an integer, and the input ports switch the beams. Each beam has spatial orthogonality. Since a Butler matrix can be composed of only passive elements, it has a lower insertion loss than other active beam scanning networks.

The Butler matrix offers only 1D beam switching. In order to steer two dimensionally, vertical and horizontal beam steering matrices should be cascaded [4]–[10]. In [5], a one-body 2D Butler matrix was proposed. It has low insertion loss and a simpler configuration than cascades 2D Butler matrices since waveguides are used for the transmission lines of the combined 2D Butler matrices, and the matrix is composed of 2-plane hybrid couplers, 1- and 2-plane cross couplers, and phase shifters [11], [12].

The waveguide 2-plane hybrid coupler [11] has  $2 \times 2$  ports at both sides of the coupled region as shown in Fig. 1. It can be regarded as a coupler combined with a waveguide H-plane coupler [13]–[15] and an E-plane coupler [16], [17]

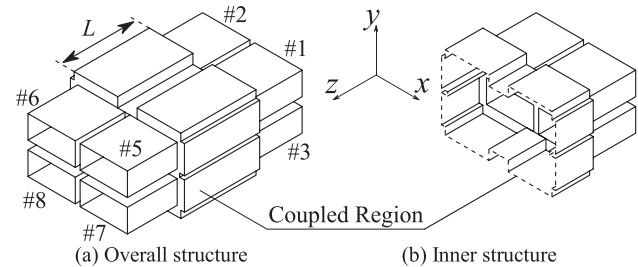


Fig. 1 Waveguide 2-plane coupler.

functionally. The ideal operation of this coupler is as follows: Taking the example of a wave incident from Port 1, Ports 1–4 have no outputs and Ports 5–8 have an amplitude of a quarter of the input, respectively. Ports 6 and 7 have 90-deg. delays and Port 8 has a 180-deg. delay in comparison with Port 5. A beam radiating from these four ports is tilted two-dimensionally, and the four input ports switch the beam directions. This makes it possible for the 2-plane hybrid coupler to be considered a  $4 \times 4$  waveguide 2D Butler matrix.

All of the radiation aperture distances need to be changed to control the beam direction. However, the positions of the ports cannot be changed because they alter the coupling characteristics of modes in the coupled region of the coupler and deteriorate properties as a 2-plane hybrid coupler. Reflection characteristics also need to be considered changing the position and the size of the ports.

In this paper, plates for controlling the beam directions of the waveguide 2-plane hybrid coupler are designed. We design the control plates individually for each plane direction, and evaluate their performance. The types of beams of the plate applied for the performance evaluation are as follows: a strongly tilted beam in the quasi E-plane, a small tilted beam in the quasi E-plane, a strongly tilted beam in the quasi H-plane, and a small tilted beam in the quasi H-plane.

## 2. Antenna Configuration

The proposed control plate and the 2-plane hybrid coupler are as shown in Fig. 2. The basic structure of the waveguide 2-plane hybrid coupler is designed by mode matching/FEM hybrid analysis [18]. The design parameters in Fig. 2 are listed in Table 1.

The beam radiation of the conventional waveguide 2-plane hybrid coupler is affected by diffracted waves at its edges. The edges are rounded to suppress the diffraction.

Manuscript received September 1, 2021.

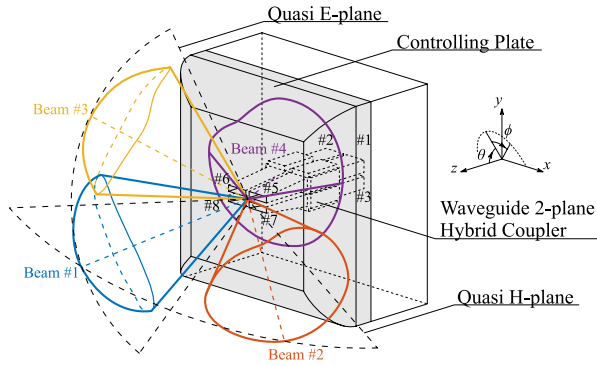
Manuscript revised December 26, 2021.

Manuscript publicized February 10, 2022.

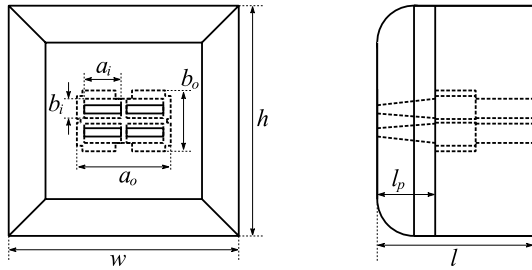
<sup>†</sup>The authors are with the Department of Electrical and Electronic Engineering, Tokyo Institute of Technology, Tokyo, 152-8552 Japan.

a) E-mail: sunaguchi@antenna.ee.titech.ac.jp

DOI: 10.1587/transcom.2021EBP3143



(a) Bird view



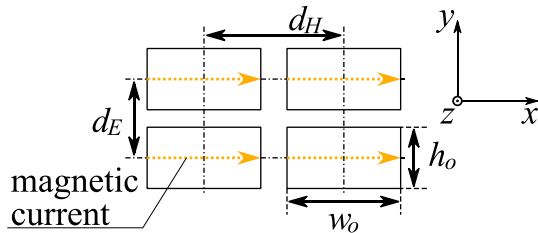
(b) Front view

(c) Side view

**Fig. 2** Waveguide 2-plane hybrid coupler and control plate.

**Table 1** Design parameters of the waveguide 2-plane hybrid coupler (unit [mm]).

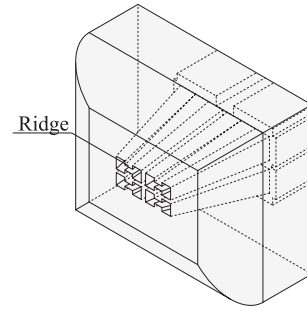
$l$	$w$	$h$	$a_i$	$b_i$
17.0	25.0	25.0	2.67	1.40
$a_o$	$b_o$	$l_p$		
3.41	2.16	6.33		


**Fig. 3** Aperture design parameters and the equivalent magnetic current of the control plate.

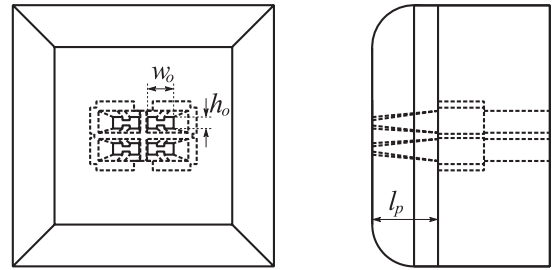
Taper waveguides are set on the output port side instead of on the original rectangular waveguide port to suppress reflections maintaining the coupling condition of the hybrid. When the aperture spacings are  $d_E$  and  $d_H$  in the vertical and horizontal directions, as shown in Fig. 3, the beam direction  $(\theta, \phi)$  satisfies the following two equations:

$$d_H \cos \theta \sin \phi = \frac{\lambda}{4} \quad (1)$$

$$d_E \sin \theta = \frac{\lambda}{4} \quad (2)$$



(a) Bird eye view



(b) Front view

(c) Side view

**Fig. 4** Ridged waveguide apertures in the plate for control in the quasi H-plane by narrower dH apertures.

where  $\lambda$  is the wavelength in free space.

By changing the control plate,  $\theta$  in the quasi E-plane and  $\phi$  in the quasi H-plane can be controlled almost independently.

### 3. Simulation Results

Table 2 details the design parameters and the simulated performance such as peak direction and beam width for each beam of the 2-plane hybrid coupler with the control plate. The design frequency of this coupler and the plate is 66.425 GHz. The values in parentheses are calculated from array factors when  $2 \times 2$  magnetic currents whose lengths are equal to the width  $w_o$  of the apertures are arranged. The distances of each of the magnetic currents are  $d_E$  and  $d_H$  as shown in Fig. 3 and the magnetic currents are assumed to have the phase difference produced by the 2-plane hybrid coupler. When a magnetic current distribution  $M_s$  is placed along the  $x$  axis, the  $E_\theta$  component of the electric field is calculated from the following equation:

$$\begin{aligned} E_\theta &= -jk_0 \frac{M_s}{4\pi} \frac{e^{-jk_0 r'}}{r'} \cos \phi \\ &\cong -jk_0 \frac{M_s}{4\pi} \frac{e^{-jk_0(r-x \sin \phi)}}{r} \cos \phi \end{aligned} \quad (3)$$

where

$k_0$  wave number in free space,

$r'$  distance between the magnetic current element and the observation point,

$r$  distance between the origin and the observation point,

**Table 2** Design parameters and simulated performance of the control plates.

aperture spacing	Plate with the conventional rectangular ports	Plate for control in the quasi E-plane		Plate for control in the quasi H-plane		
	default	wider	narrower	wider	narrower (w/ polycarbonate)	narrower (ridged waveguide)
$d_E$ [mm]	1.85	2.40	1.21	1.85	1.85	1.21
$d_H$ [mm]	3.06	3.06	3.06	3.40	1.80	1.61
$w_o$ [mm]	2.67	2.67	2.67	2.67	2.26	1.41
$h_o$ [mm]	1.40	1.40	0.60	1.40	1.40	0.80
Peak direction in quasi E-plane [deg]	32 (37)	26 (28)	54 (69)	30 (37)	43 (38)	38
Peak direction in quasi H-plane [deg]	16 (16)	16 (16)	16 (15)	15 (19)	29 (38)	32
Beam width in quasi E-plane [deg]	65 (83)	57 (64)	60	66 (84)	60 (89)	57
Beam width in quasi H-plane [deg]	34 (38)	35 (38)	36 (38)	32 (32)	49 (50)	65

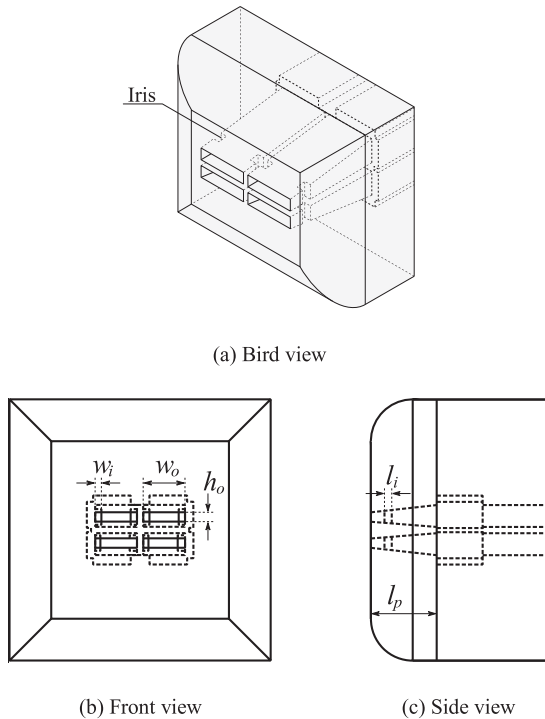


**Fig. 5** Waveguide with irises in the plate for control in the quasi E-plane by narrower dE apertures.

$x$  distance between the origin and the magnetic current element,  
 $\phi$  crossing angle between the corresponding vectors to  $x$  and  $r'$ .  
 The magnetic current distribution  $M_s$  in the waveguide aper-

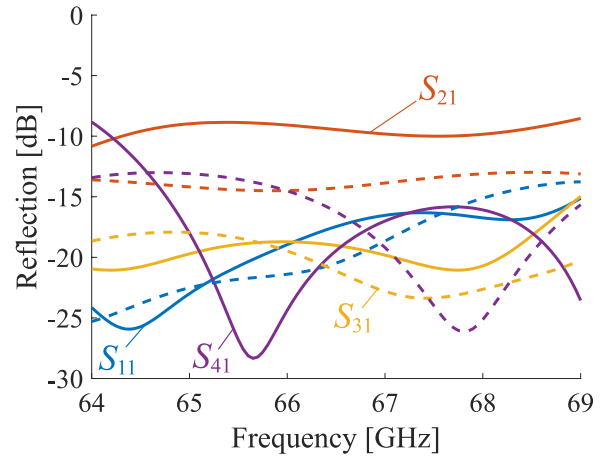


**Fig. 6** Frequency characteristics of the scattering matrix on the input side in the waveguide 2-plane hybrid coupler with the plate for control in the quasi E-plane (dashed line: conventional rectangular waveguide port, solid line: narrower dE aperture spacing).

**Table 3** Design parameters of the plate with the ridged waveguide apertures (unit [mm]).

$w_o$	$h_o$	$l_p$
1.41	0.80	6.33

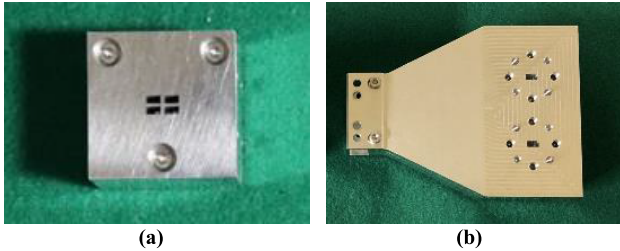
ture whose width is  $w_o$  is assumed to be

$$M_s = M_0 \cos\left(\frac{\pi x}{w_o}\right) \tag{4}$$

then  $E_\theta$  of each single waveguide aperture can be calculated as

**Table 4** Design parameters of the plate with the waveguide apertures with irises (unit [mm]).

$w_o$	$h_o$	$w_i$	$l_i$	$l_p$
2.67	0.60	0.35	0.40	6.33


**Fig. 7** Fabricated (a) waveguide 2-plane hybrid coupler and (b) transition unit from a WR15 waveguide port to the input port of the waveguide 2-plane hybrid coupler.

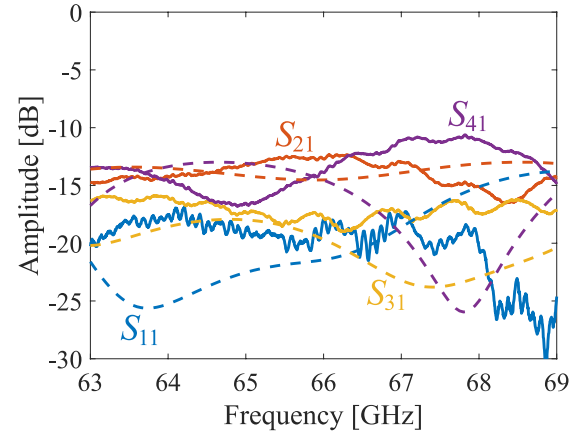
**Table 5** Peak direction and gain of measured beam pattern.

	The plate with the conventional rectangular port	The plate for control in the quasi E-plane by narrower dE apertures
Peak direction in quasi E-plane [deg]	21	53
Peak direction in quasi H-plane [deg]	17	16
Gain [dBi]	10.5	11.3

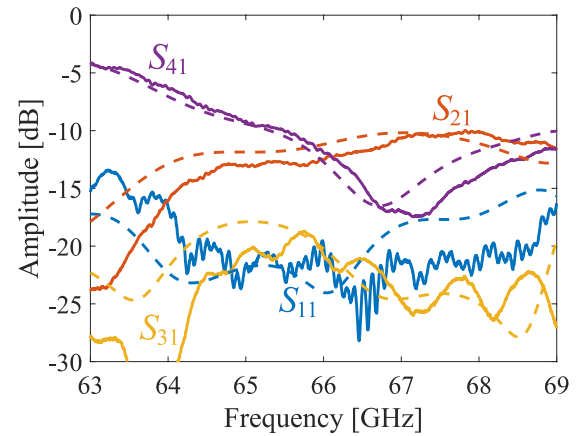
$$\begin{aligned}
 E_{\theta} &= \int_{-\frac{w_o}{2}}^{\frac{w_o}{2}} -jk_0 \frac{M_0 \cos\left(\frac{\pi x}{w_o}\right)}{4\pi} \frac{e^{-jk_0(r-x \sin \phi)}}{r} \cos \phi dx \\
 &= \frac{-\frac{2\pi}{w_o} \cos \phi}{(k_0 \sin \phi)^2 - \left(\frac{\pi}{w_o}\right)^2} e^{-jk_0 r} \cos\left(\frac{k_0 w_o}{2} \sin \phi\right) \quad (5)
 \end{aligned}$$

The array factor of the magnetic currents in the control plate can be calculated by summing up the radiated electric fields considering the phase differences and the position offsets. The array factors do not consider diffractions at the edges of the plate. The original coupler has rectangular  $2.67 \times 1.40$  mm waveguide ports and the beam directions are  $\pm 32$  deg and  $\pm 16$  deg in the quasi E-plane and the quasi H-plane, respectively.

The plate can change the beam direction in the range of  $\pm 15$ – $32$  deg. for the quasi H-plane control. When the tilt angle is large, the aperture spacing must be small. However, the width of the waveguide port cannot be wide enough to be able to avoid stay inside its cutoff frequency. There are two methods proposed for reducing the cutoff frequency of the control plate. One is filling the taper waveguides of the plate with polycarbonate. The other is introducing ridges on the top and bottom walls at the output ports as suggested in Fig. 4. The design parameters of this plate are shown in Table 3. The plate with the ridged waveguides has a slightly larger tilt angle than that with polycarbonate. However, the



(a)



(b)

**Fig. 8** Frequency characteristics of the scattering matrix on the input side in the waveguide 2-plane hybrid coupler with the control plate (a) The plate with original rectangular port, (b) The plate with narrower dE apertures (solid line: measured results, dashed line: simulated results).

beam width of the plate with the ridged waveguides are wider than that with polycarbonate.

The plate can change the direction in a range of  $\pm 26$ – $54$  deg. for the quasi E-plane control. When the tilt angle is large, the impedance of the apertures is reduced because the height of the apertures must be small to shorten the aperture spacing. Inductive irises are introduced to the tapered waveguides in the plate with beam direction  $\pm 54$  deg in the quasi E-plane to match the impedance of the apertures and the wave impedance as shown in Fig. 5. The design parameters are listed in Table 4. The frequency characteristics of the scattering matrix in the input side in the coupler and the plate for the quasi E-plane control are shown in Fig. 6. For a plate having the narrower aperture spacing,  $S_{41}$  is suppressed less than  $-20$  dB at  $65.1$ – $66.4$  GHz. However,  $S_{21}$  becomes larger than  $-10$  dB at frequencies higher than  $64.3$  GHz. This is caused by the mutual coupling between Ports 5 and 7, or 6 and 8. The tilt angle cannot be larger than  $\pm 54$  deg in the

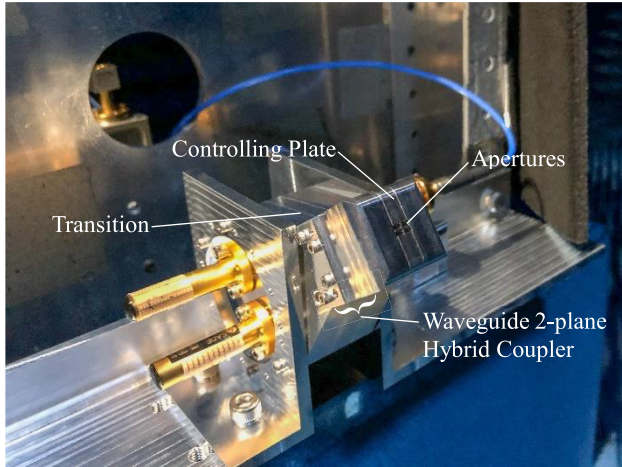


**Fig. 9** Far field measurements of the fabricated waveguide 2-plane hybrid coupler and control plate.

quasi E-plane because of this mutual coupling.

#### 4. Experimental Results

Based on the simulated results, the waveguide 2-plane hybrid coupler and the control plate with the conventional rectangular waveguide ports and the plate for controlling in the quasi E-plane by narrower dE apertures were fabricated. The material of all these devices is aluminum(A6061). The fabricated waveguide 2-plane hybrid coupler is shown in Fig. 7(a). The size of the coupler is  $25.0 \times 25.0 \times 17.0$  mm, and its weight is only 28 g. For connecting the input port of this coupler to a standard WR15 waveguide, a transition unit is also fabricated as shown in Fig. 7(b). Figure 8 shows the measured frequency characteristics of the scattering matrix on the input side in the waveguide 2-plane hybrid coupler with the control plates. Due to manufacturing errors, the measured results of the control plate with the conventional rectangular waveguide ports disagree slightly with the simulated results. However, the measured scattering matrix is within  $-12.2$  dB at the design frequency. The measured characteristics of the narrower dE control plate agrees well with the simulated results however. They are below  $-11.8$  dB at the design frequency.

The radiation patterns were measured in an anechoic chamber as shown in Fig. 9. In this picture, the coupler is tilted so that the quasi H-plane faces in the horizontal direction. The coupler and its measurement system rotates horizontally and the quasi H-plane beam pattern can be obtained. If the coupler is mounted so that the quasi E-plane is oriented to the horizontal direction, and the quasi E-plane beam pattern can be measured. The radiation patterns in the quasi E-plane and the quasi H-plane of each control plate are shown in Figs. 10 and 11. Considering the symmetry, only the beams from Ports 1 and 2 are measured. The peak direction and gain of each beam pattern are listed in Table 5. Due to the ripples in the measured pattern and the gain reduction in the quasi E-plane of the 2-plane waveguide

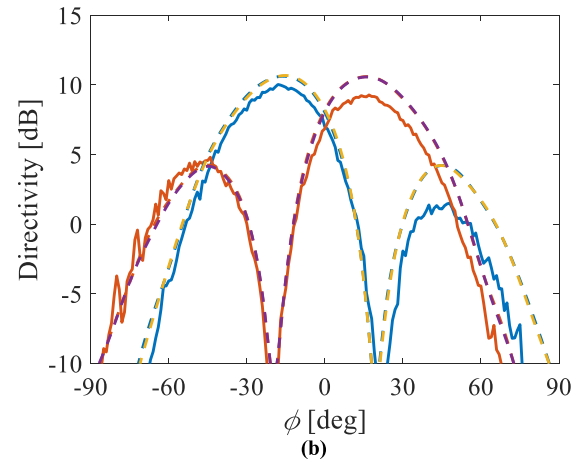
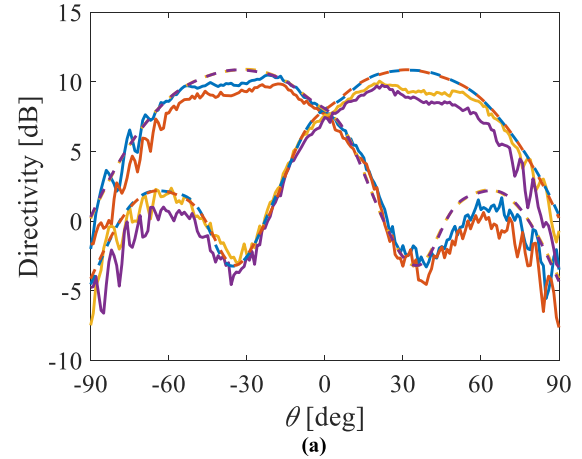


**Fig. 10** Radiation characteristics of the 2-plane waveguide coupler with the conventional rectangular port: (a) Radiation for the quasi E-plane at 66.43 GHz, (b) Radiation for the quasi H-plane at 66.43 GHz (solid line: measured results, dashed line: simulated results).

coupler with the conventional rectangular port arising from manufacturing errors, the simulated and measured results show differences. However, the approximate shapes of the simulation and measurement directivities agree well.

Table 6 summarizes and compares with other similar work available in the literature in terms of frequency, transmission line, configuration, beams, size, and amplitude/phase error [2], [5], [9], [10], [19]–[23]. The amplitude/phase error has the largest difference between the measured and theoretical values at the design frequency. The waveguide-type matrices in this paper and [5] are somewhat bulky three-dimensionally, however, they display smaller amplitude/phase errors than microstrip/SIW-type matrices.

#### 5. Conclusions

We have designed a plate to control beam directions in the waveguide 2-plane hybrid coupler. The radiation direction can be changed in both the quasi H-plane and the quasi E-plane. The coupler and the plates with the original rectangular waveguide ports and with the narrower dE apertures were

**Table 6** Reported results with other work.

Ref.	Frequency	Transmission line	Configuration	Beams	Size ( $\lambda^3$ )	Amplitude/phase error
[19]	2.4 GHz	Microstrip	2-D Butler matrix	4 x 4	1.6 x 1.6 x 0.004	1.2dB/7°
[20]	28 GHz	Microstrip	8 Butler matrices	4 x 4	3.3 x 5.9 x 0.02	N.A.
[21]	10 GHz	SIW	2-D Bulter matrix	4 x 4	22.0 x 16.7 x 0.03	2.6dB/17°
[10]	30 GHz	SIW	8 Butler matrices	4 x 4	16.5 x 4.5 x 0.2	2.4dB/10°
[22]	30 GHz	SIW	2-D Butler matrix	2 x 4	23.5 x 19.4 x 0.05	N.A.
[9]	60 GHz	SIW	8 Butler matrices	4 x 4	30.0 x 30.0 x 0.7	N.A.
[23]	94 GHz	SIW	2 folded Butler matrices and four hybrid couplers	2 x 4	6.8 x 5.3 x 0.5	0.7dB/8°
[5]	22 GHz	Waveguide	2-D Butler matrix	2 x 2	3.3 x 3.3 x 2.1	0.6dB/8°
This work	66 GHz	Waveguide	2-D Butler matrix	2 x 2	5.5 x 5.5 x 3.8	0.3dB/1°

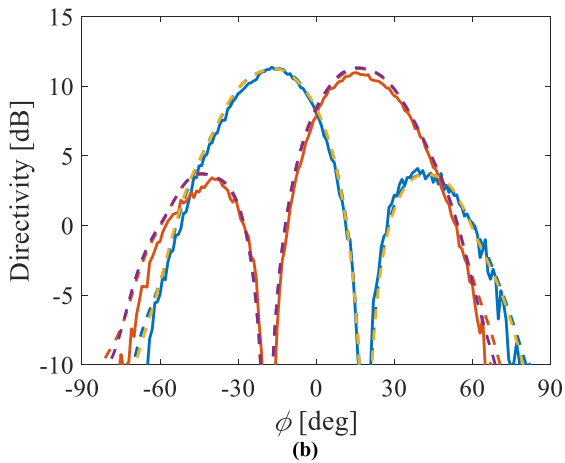
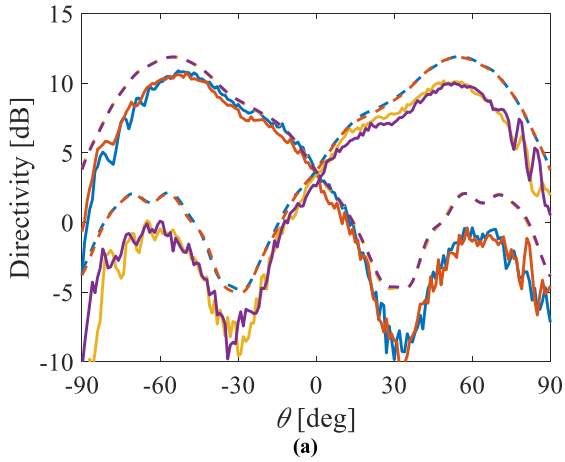


**Fig. 11** Radiation characteristics of the 2-plane waveguide coupler with the plate for control in the quasi E-plane by narrower dE apertures: (a) Radiation for the quasi E-plane at 66.43 GHz, (b) Radiation for the quasi H-plane at 66.43 GHz (solid line: measured results, dashed line: simulated results).

fabricated and measured. Good agreement was observed between the evaluation results of the fabricated plates and the

simulated results. At the design frequency of 66.43 GHz, the peak directions in the quasi E-plane of the plate with the original rectangular ports and the narrower dE control plate were measured to be 21 deg. and 53 deg., respectively, while those in the quasi H-plane were very similar. At this frequency, the maximum reflections in the waveguide 2-plane hybrid coupler with the plates were -12.2 dB and -11.8 dB, respectively.

**Acknowledgments**

This work is supported in part by the Strategic Information and Communication R&D Promotion Programme (185004002) of the Ministry of Internal Affairs and Communications in Japan.

**References**

- [1] R.H. Roy, "Spatial division multiple access technology and its application to wireless communication systems," *IEEE Vehicular Techn. Conf.*, vol.2, pp.730-734, May 1997.
- [2] E.G. Larsson, O. Edfors, F. Tufvesson, and T.L. Marzetta, "Massive MIMO for next generation wireless systems," *IEEE Commun. Mag.*, vol.52, no.2, pp.186-195, Feb. 2014.
- [3] L. Lu, G.Y. Li, A.L. Swindlehurst, A. Ashikhmin, and R. Zhang, "An overview of massive MIMO: Benefits and challenges," *IEEE J. Sel. Topics Signal Process.*, vol.8, no.5, pp.742-758, Oct. 2014.
- [4] K. Nishimori, "Novel technologies using massive MIMO transmission toward 5G and its beyond system," *Intl. Symp. Antennas Propag., WeG1-1*, Oct. 2018.
- [5] D.-H. Kim, J. Hirokawa, and M. Ando, "Design of waveguide short-slot two-plane couplers or one-body 2-D beam-switching butler matrix application," *IEEE Trans. Microw. Theory Techn.*, vol.64, no.3, pp.776-784, March 2016.
- [6] J.H. Acoraci, "Practical implementation of large Butler matrices," *US Patent 4,356,461*, Oct. 1982.
- [7] Y.J. Cheng, W. Hong, and K. Wu, "A two-dimensional multibeam array antenna based on substrate integrated waveguide technology," *Asia-Pacific Microw. Conf.*, DOI: 10.1109/APMC.2008.4958075, Dec. 2008.
- [8] W. Chen, M.-H. Huang, P.-Y. Lyu, S. Chang, and C. Chang, "A 60-GHz CMOS 16-beam beamformer for two-dimensional array antennas," *IEEE MTT-S Intl. Microw. Symp.*, DOI: 10.1109/MWSYM.2014.6848453, June 2014.

- [9] Y. Li, J. Wang, and K. Luk, "Millimeter-wave MultiBeam aperture-coupled magnetoelectric dipole array with planar substrate integrated beamforming network for 5G applications," *IEEE Trans. Antennas Propag.*, vol.65, no.12, pp.6422–6431, Dec. 2017.
- [10] J. Lian, Y. Ban, Q. Yang, B. Fu, Z. Yu, and L. Sun, "Planar millimeter-wave 2-D beam-scanning multibeam array antenna fed by compact SIW beam-forming network," *IEEE Trans. Antennas Propag.*, vol.66, no.3, pp.1299–1310, March 2018.
- [11] D.-H. Kim, J. Hirokawa, and M. Ando, "One-body 2-D beam-switching butler matrix with waveguide short-slot 2-plane couplers," *IEICE Trans. Electron.*, vol.E100-C, no.10, pp.884–892, Oct. 2017.
- [12] T. Tomura, D.-H. Kim, M. Wakasa, Y. Sunaguchi, J. Hirokawa, and K. Nishimori, "A 20-GHz-band 64×64 hollow waveguide two-dimensional butler matrix," *IEEE Access*, vol.7, pp.164080–164088, Nov. 2019.
- [13] H.J. Riblet, "The short-slot hybrid junction," *Proc. IRE*, vol.40, no.2, pp.180–184, Feb. 1952.
- [14] L.T. Hildebrand, "Results for a simple compact narrow-wall directional coupler," *IEEE Microw. Guid. Wave Lett.*, vol.10, no.6, pp.231–232, June 2000.
- [15] S. Yamamoto, J. Hirokawa, and M. Ando, "Length reduction of a short-slot directional coupler in a single-layer dielectric substrate waveguide by removing dielectric near the side walls of the coupler," *IEEE Antennas Propag. Symp.*, vol.3, pp.2353–2356, June 2004.
- [16] T. Kawai, M. Kishihara, Y. Kokubo, and I. Ohta, "Cavity-type directional couplers with simple structure," *IEEE Intl. Microw. Symp.*, vol.2, pp.413–416, June 1997.
- [17] Y. Zhang, Q. Wang, and H. Xin, "A compact 3 dB E-plane waveguide directional coupler with full bandwidth," *IEEE Microw. Wirel. Compon. Lett.*, vol.24, no.4, pp.227–229, April 2014.
- [18] M. Wakasa, D.-H. Kim, T. Tomura, and J. Hirokawa, "Wideband design of a short-slot 2-plane coupler by the mode matching/FEM hybrid analysis considering the structural symmetry," *IEICE Trans. Commun.*, vol.E102-B, no.5, pp.1019–1026, May 2019.
- [19] K. Ding, and A.A. Kishk, "2-D butler matrix and phase-shifter group," *IEEE Trans. Microw. Theory Techn.*, vol.66, no.12, pp.5554–5562, Dec. 2018.
- [20] X. Wang, X. Fang, M. Laabs, and D. Plettemeier, "Compact 2-D multibeam array antenna fed by planar cascaded butler matrix for millimeter-wave communication," *IEEE Antennas Wireless Propag. Lett.*, vol.18, no.10, pp.2056–2060, Oct. 2019.
- [21] J.-W. Lian, Y.-L. Ban, H. Zhu, and Y.J. Guo, "Uniplanar beam-forming network employing eight-port hybrid couplers and crossovers for 2-D multibeam array antennas," *IEEE Trans. Microw. Theory Techn.*, vol.68, no.11, pp.4706–4718, Nov. 2020.
- [22] C. Bartlett and J. Bornemann, "Cross-configuration substrate integrated waveguide beamforming network for 1D and 2D beam patterns," *IEEE Access*, vol.7, pp.151827–151835, Oct. 2019.
- [23] W. Yang, Y. Yang, W. Che, C. Fan, and Q. Xue, "94-GHz compact 2-D multibeam LTCC antenna based on multifolded SIW beam-forming network," *IEEE Trans. Antennas Propag.*, vol.65, no.8, pp.4328–4333, Aug. 2017.



**Yuki Sunaguchi** received the B.S. and M.S. degrees in electrical and electronic engineering from Tokyo Institute of Technology in 2018 and 2020, respectively. He is currently working for Murata Manufacturing Co., Ltd.



**Takashi Tomura** received the B.S., M.S. and D.E. degrees in electrical and electronic engineering from the Tokyo Institute of Technology, Tokyo, Japan, in 2008, 2011 and 2014, respectively. He was a Research Fellow of the Japan Society for the Promotion of Science (JSPS) in 2013. From 2014 to 2017, he worked at Mitsubishi Electric Corporation, Tokyo and was engaged in research and development of aperture antennas for satellite communications and radar systems. From 2017 to 2019, He was a Specially Appointed Assistant Professor at the Tokyo Institute of Technology, Tokyo. He is currently an Assistant Professor there. His research interests include electromagnetic analysis, aperture antennas and planar waveguide slot array antennas. Dr. Tomura received the Best Student Award from Ericsson Japan in 2012 and the IEEE AP-S Tokyo Chapter Young Engineer Award in 2015 and Young Researcher Award from IEICE technical committee on antennas and propagation in 2018. He is a member of the IEEE.



**Jiro Hirokawa** was born in Tokyo, Japan in 1965. He received the B.S., M.S., and D.E. degrees in electrical and electronic engineering from Tokyo Institute of Technology (Tokyo Tech), Tokyo, Japan in 1988, 1990, and 1994, respectively. He was a Research Associate from 1990 to 1996 and an Associate Professor from 1996 to 2015 at Tokyo Tech. He is currently a Professor there. He was with the antenna group of Chalmers University of Technology, Gothenburg, Sweden, as a Postdoctoral Fellow from 1994 to 1995. His current research interests include analyses, designs, and fabrication techniques of slotted waveguide array antennas, millimeter-wave, and Terahertz antennas, and beam-switching circuits. He has authored or co-authored more than 200 peer-reviewed journal papers and more than 600 international conference presentations. He served as an Associate Editor for *IEICE Transactions on Communications* during terms of 1999–2003 and 2004–2007. He also served as an Associate editor from 2013–2016 and is currently serving as a Track Editor for *IEEE Transactions on Antennas and Propagations* since 2016. He was the chair of the technical program committee for ISAP 2016. He was also the chair of IEICE technical committee on Antennas and Propagation from 2017 to 2019. He received IEEE AP-S Tokyo Chapter Young Engineer Award in 1991, Young Engineer Award from IEICE in 1996, Tokyo Tech Award for Challenging Research in 2003, Young Scientists' Prize from the Minister of Education, Cultures, Sports, Science and Technology in Japan in 2005, Best Paper Award in 2007 and a Best Letter Award in 2009 from IEICE Communications Society, and IEICE Best Paper Award in 2016 and 2018. He is a Fellow of IEICE and IEEE.